J Mater Sci: Mater Med (2011) 22:797–807
DOI 10.1007/s10856-011-4282-y

Corrosion behaviour of heat treated boron free and boron containing Ti–13Zr–13Nb (wt%) alloy in simulated body fluid

P. Majumdar · S. B. Singh · U. K. Chatterjee · M. Chakraborty

Received: 10 September 2010 / Accepted: 7 March 2011 / Published online: 26 March 2011

Abstract The corrosion behaviour of heat treated Ti–13Zr–13Nb (TZN) and Ti–13Zr–13Nb–0.5B (TZNB) alloys in Hank's solution has been investigated. The microstructure of the heat treated TZN alloy consisted of α, β or martensite. Addition of boron to TZN alloy led to the formation of dispersed TiB particles and modification of microstructure. In general, the furnace cooled TZN sample showed lower corrosion potential (E_{corr}) than the air cooled sample. Aging of water quenched samples decreased the E_{corr} value. The passive current density of TZN samples varied within a narrow range. Presence of boron in TZN alloy decreased the corrosion potential and substantially increased the passive current density. Results showed that boron deteriorated the corrosion resistance of TZN alloy.

1 Introduction

Corrosion is one of the most important parameters in determining the suitability of a material for biomedical applications. Corrosion of metallic biomaterials is a two-fold problem. On one hand, it leads to degradation of material and on the other hand, it releases ions that can adversely influence the function of the organism, cause inflammatory response and sometimes lead to the formation of foreign body giant cells [1]. The corrosion behavior of materials is controlled by the presence of protective oxide films over the surface. Corrosion resistant materials react easily with oxygen from the atmosphere and form a surface oxide layer, the so called passive layer, which acts as a barrier against further reaction [1, 2]. The biological response of the implants is influenced by the chemical composition of the biomaterials and stability of their surface oxide layer because the surface of biomaterials is in direct contact with biological tissues [3].

Among the conventional metallic biomaterials, titanium and its alloys are found to offer higher corrosion resistance than Co–Cr alloys and 316L stainless steel in several media including human body due to the presence of a dense and thermodynamically stable TiO_2 layer on the surface. This layer can spontaneously reform after being damaged, even in solutions with low oxygen contents [4, 5]. The corrosion behaviour of titanium alloys varies with the alloy composition, environment, heat treatment conditions and microstructure [6]. Aparicio et al. [7] have shown that the roughness does not influence the corrosion potential (E_{corr}) values of commercially pure titanium. Reactive metals such as Ta, Nb or Zr behave in the same way as titanium. Addition of Zr, Nb and Ta to titanium alloys stabilizes the surface oxide films in human body environment and improves corrosion resistance [4] and accordingly, the rate of titanium ion release in five mass% HCl solution was found to decrease with increasing quantities of Zr, Nb and Ta [8]. The presence of Zr in the α phase and Nb in the β phase leads to the high corrosion resistance of both the phases of the 'near-β' Ti–13Zr–13Nb alloy [8, 9]. This is associated with the formation of ZrO_2 and Nb_2O_5 that strengthen the TiO_2 passive film formed on the surface of this alloy [9, 10]. Similarly, the high corrosion resistance of the Ti–15Zr–4Nb–4Ta alloy can be attributed to the presence of passive film that consists mainly of TiO_2, with trace

P. Majumdar (✉) · S. B. Singh · U. K. Chatterjee · M. Chakraborty
Department of Metallurgical and Materials Engineering, Indian Institute of Technology, Kharagpur, India
e-mail: m.pallab@gmail.com

Present Address:
M. Chakraborty
Indian Institute of Technology, Bhubaneswar, India

quantities of Ti_2O_3, ZrO_2, Nb_2O_5 and Ta_2O_5 [11]. Khan et al. [12] have reported that $\alpha + \beta$ titanium alloys (Ti–6Al-4V and Ti–6Al–7Nb) possess a good combination of corrosion and wear resistance whereas the commercially pure titanium and near β (Ti–13Zr–13Nb) and β (Ti–15Mo) alloys showed only excellent corrosion resistance. Khan et al. [13] have also shown that Ti–13Zr–13Nb alloy possesses better corrosion resistance properties compared to CP titanium and Ti–15Mo alloys in phosphate buffer saline (PBS) solution at three different pH values. Oliveira et al. [14] have noticed that the Ti–13Zr–13Nb alloy has better corrosion resistance than the Ti–50Zr alloy. Passivity of the Ti–6Al-4V alloy in Ringer's solution was obtained in the potential range of −400 to +1400 mV versus saturated calomel electrode (SCE) [15]. Similarly, anodic polarization studies on Ti–6Al–7Nb, Ti–6Al-4V and cp-Ti in deaerated Ringer's solution showed passivity in the potential range of 0 to 2200 mV (SCE) with the primary passive current density at ~ 10 μA/cm^2 [15].

Titanium and several of its alloys are used as traditional biomaterials because of their excellent combination of corrosion resistance, biocompatibility and mechanical properties [16–18]. However, poor tribological properties of titanium and its alloys reduce the service life of the implants significantly in articulating conditions. Therefore, the recent focus has been on improving the wear resistance by proper surface modification techniques and/or by reinforcing the matrix with some hard precipitates [18]. Reinforcing the soft matrix of titanium alloys (including new generation β-Ti alloys) with hard ceramic precipitates such as borides offers the possibility of substantially enhancing the wear resistance of these composites [19]. Small addition of boron to titanium alloys leads to the formation of strong and stiff titanium-boride (TiB) phase that precipitates in situ during solidification [20, 21]. However, the effect of boron on corrosion behaviour of titanium alloys needs to be investigated in order to assess the suitability of the implant in the body environment. Also, the corrosion properties of the alloys are affected by the changes in microstructure brought about by heat treatment and therefore, should be clearly understood *vis-à-vis* microstructures.

The present study was undertaken to investigate the effect of boron and the influence of microstructure on the corrosion behaviour of the Ti–13Zr–13Nb alloy.

2 Experimental

Ti–13Zr–13Nb (TZN) and Ti–13Zr–13Nb–0.5B (TZNB) alloys (compositions in wt%) were prepared by arc melting with a non consumable tungsten electrode in a vacuum arc melting unit supplied by *Vacuum Techniques Pvt Ltd, Bangalore*. The melting chamber was first evacuated to less than 5×10^{-4} Pascal and then flushed with high purity argon and evacuated again; the chamber was finally backfilled with the same gas. Before melting the alloy, a piece of pure titanium was melted as getter. The samples were turned over and remelted at least six times in order to attain homogeneity in composition and microstructure. Three or four small buttons were remelted together and cast into ingot (approx. 40 g) in the same melting unit.

The β transition temperature of TZN alloy has been reported to be 740°C [22]. Based on this transition temperature, the heat treatment was performed on TZN. It was assumed that the addition of only 0.5 wt% boron to the TZN alloy would not change the transformation temperature substantially. Hence, the same heat treatment schedule which was applied on TZN alloy was maintained for TZNB alloy.

The ingot was given 30–40% reduction by hot rolling at two different temperatures (800 and 650°C) and then air cooled to room temperature. The hot rolling temperatures were selected in such a way that it was above the β transition temperature in one case (800°C) and below that temperature in another (650°C). The hot rolled TZN samples were solution treated at 800, 700 and 650°C for 1 h in dynamic argon atmosphere; this was followed by furnace cooling (FC), air cooling (AC) or water quenching (WQ). Water quenched samples were aged at 500°C for 5 h (Aged). However, in case of TZNB samples that were hot rolled at 650°C, the solution treatment was done at 650°C only and the low temperature (650°C) solution treated samples were cooled in two different rates i.e. air cooled and water quenched. Figure 1 schematically represents the heat treatment schedule of TZN and TZNB alloy.

The average composition of the alloys was determined by using scanning electron microscopy-energy dispersive spectroscopy (SEM–EDS) on a scanning electron microscope (SEM) (Model: JSM-5800, JEOL, Japan), attached with Energy Dispersive X-ray (Model: ISIS 300 Oxford Instruments Limited, UK). The operating voltage of the

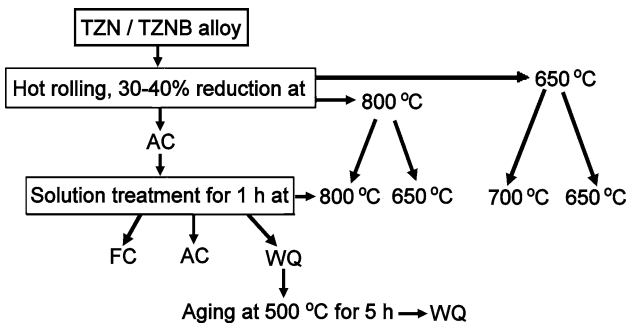

Fig. 1 Schematic diagram illustrating the thermomechanical treatment of TZN and TZNB alloys

SEM was 20 kV. For chemical analysis of the alloys, a number of regions were examined for each alloy in order to have an average composition. In case of alloys containing boron, the composition was scaled to Ti + Zr + Nb = 100 wt% as suggested by Samuel et al. [19], because, the boron content in the alloy cannot be quantified by EDS. In addition, interstitial gas analyses were carried out using Laboratory Equipment Corporation (LECO) analyzers in *Wah Chang lab*, *USA* in order to measure the oxygen, nitrogen, hydrogen and carbon content of the alloys.

Optical microscopy was used for microstructural examination of the heat treated samples. The polished samples were etched with Kroll's reagent (10 vol% HF and 5 vol% HNO_3 in water). For SEM studies, the microstructures were examined on scanning electron microscope, FEI Quanta ESEM operating at 20 kV and FEI Nova Nanolab 200 with FEG-SEM column operating at 20 kV using the secondary electron (SE) and backscattered electron (BSE) imaging modes. Hardness of the pre-polished samples was measured at 10 kg load using a Vickers hardness tester.

Corrosion behaviour of the titanium alloys was evaluated at room temperature (30°C) in Hank's solution. Freshly prepared Hank's solution was used for each experiment. The solution had the following chemical composition dissolved in 1 l of distilled water: 8 g NaCl, 1 g glucose, 0.4 g KCl, 0.35 g $NaHCO_3$, 0.14 g $CaCl_2$, 0.1 g $MgCl_2{\cdot}6H_2O$, 0.06 g $Na_2HPO_4{\cdot}2H_2O$, 0.06 g KH_2PO_4 and 0.06 g $MgSO_4{\cdot}7H_2O$ [3, 23]. The pH of the solution was maintained at 7.4. The medium was deaerated with high purity nitrogen gas 15 min before starting the experiment; deaeration was continued during the experiment in order to remove any dissolved oxygen from the solution. The concentration of oxygen in body liquid of muscle tissues, except blood, is rather small [6]. The dissolved oxygen content in a living body is known to be about 20% of that of the atmosphere [4]. However, the present work was conducted under a deaerated, high purity nitrogen atmosphere in order to lower the oxygen concentration in the solution to create a severe environment. Freshly prepared solution was used for each experiment and specimens with mirror surface finish were used for the test. The electrical contact was made by soldering a copper wire to the back of the sample. The electrical contact as well as the untested sample areas were isolated by an insulating lacquer. Three to four samples of each group were tested.

Anodic polarization test was conducted with a computer controlled *Meinsberger Potentiostat/Galvanostat PS6* (Germany). The electrolyte cell was made of glass with a capacity of 100 ml. The sample acted as the working electrode (anode) and platinum as the counter electrode (cathode). A saturated calomel electrode (SCE) was used as a reference electrode and all the potential measurements were made with reference to it. The specimen was initially held at open circuit potential (OCP) for 600 s in order to stabilize the free corrosion potential. Polarization was started at 500 mV below the OCP and increased at a rate of 1 mV per minute towards anodic direction; it was terminated at 2000 mV above the OCP. Corrosion potential (E_{corr}) and passive current density (i_{pass}) of the alloys were determined from the potential versus current density polarization curve.

3 Results

The composition, including interstitials content, of the investigated TZN alloy with and without boron, obtained by SEM–EDS studies and LECO analysis, is given in Table 1. The average composition of the boron free and boron containing TZN alloy can be expressed as Ti–13Zr–13Nb and Ti–13Zr–13Nb–0.5B (wt%), respectively.

3.1 Microstructure

Depending on the heat treatment conditions, the microstructure of the heat treated TZN alloy mainly consisted of elongated/equiaxed α, β or martensite. Deformation and solution treatment above the β transus (800°C) led to the formation of Widmanstätten α laths in furnace cooled (Fig. 2a) and air cooled samples and martensite in water quenched sample (Fig. 2b). After aging of the water quenched sample fine globular α formed along the pre-existing martensite plates (Fig. 2c). Equiaxed primary α in furnace cooled and air cooled samples, and globular/elongated α and martensite in water quenched sample were found after solution treatment from 700°C. Aging treatment of water quenched sample resulted in the growth of primary α while retaining the overall morphology of the water quenched samples. In case of solution treatment at 650°C after deformation from 800 or 650°C, primary α was found after cooling from the solution treatment temperature (Fig. 3a). Martensite was not formed after water quenching due to partitioning effect of the alloying elements (Fig. 3b). Aging of the water quenched samples changed the elongated α into equiaxed α and enhanced the growth of primary α (Fig. 3c). In general, air cooling led to finer microstructure than furnace cooling.

Table 1 The chemical composition (wt%) of the alloys used in this study

Alloy	Ti	Nb	Zr	O	C	N	H
TZN	73.42	13.41	13.17	0.12	0.0122	0.0047	0.012
TZNB	73.51	13.86	12.86	–	–	–	–

Note: interstitial contents were not measured for boron containing alloy

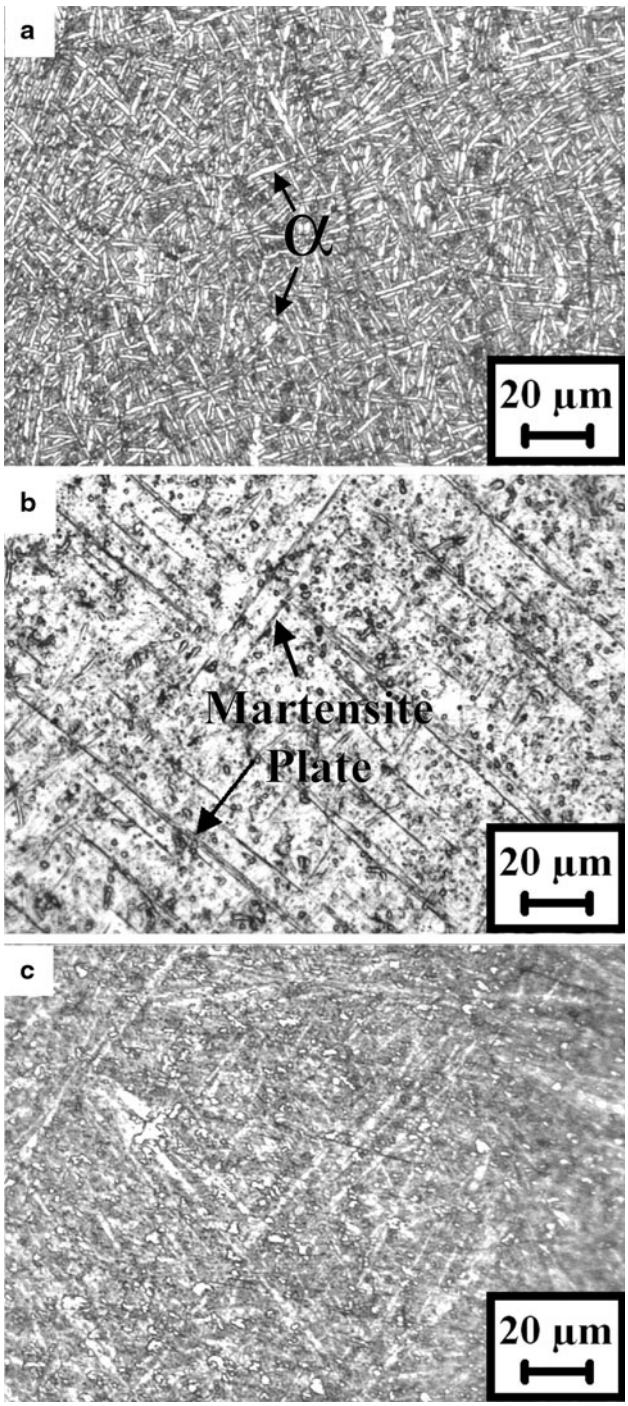

Fig. 2 Microstructures of the TZN alloy deformed and solution treated at 800°C followed by (**a**) furnace cooling, (**b**) water quenching and (**c**) aging of the water quenched sample

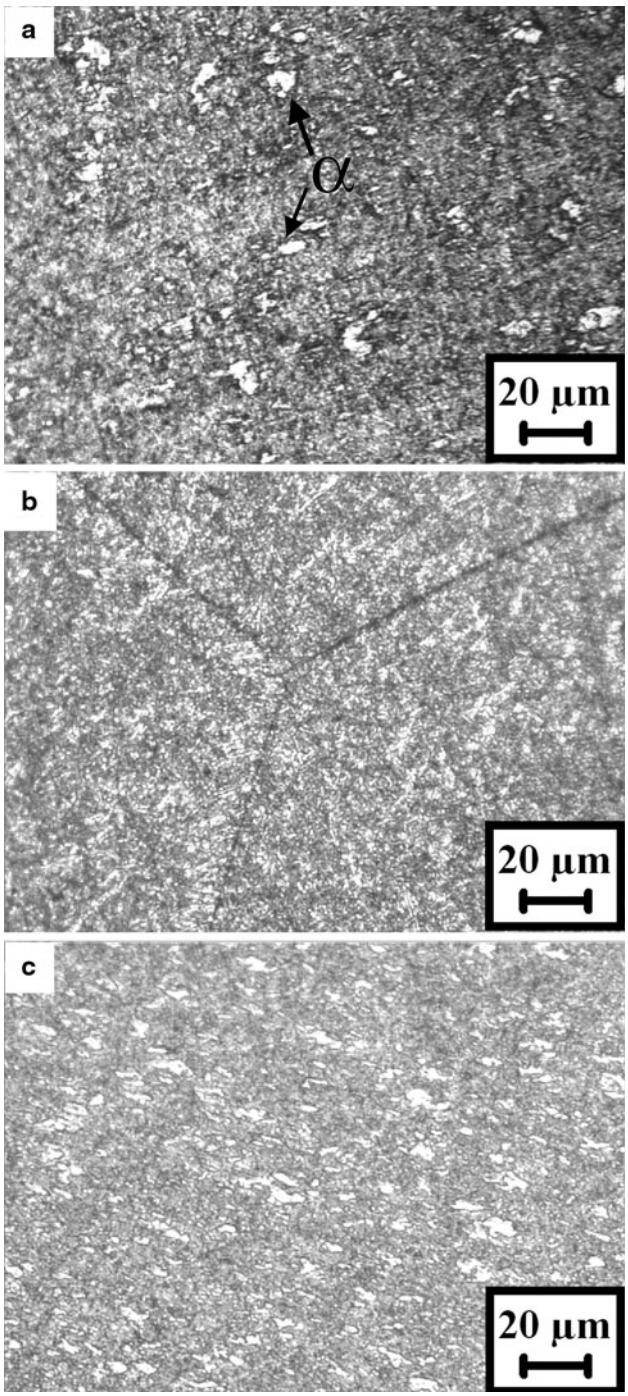

Fig. 3 Microstructures of the TZN alloy deformed and solution treated at 650°C followed by (**a**) furnace cooling, (**b**) water quenching and (**c**) aging of the water quenched sample

Addition of 0.5 wt% B to TZN alloy resulted in the formation of dispersed precipitated particles of titanium boride (TiB). The composition of the TZNB alloy corresponds to TZN + ~3.2 vol.% of TiB. The majority of the boride precipitate particles were acicular (needle like) with lengths varying in the range of 5–10 μm with some particles being even larger than that (Fig. 4). Boron had no other appreciable effect on the overall microstructure of the TZN alloy samples that were deformed and solution treated at 800°C. However, the aged sample showed some growth of the α phase. In case of TZNB alloy solution treated at 650°C after deformation at 800 or 650°C, growth of the α phase was observed in the microstructure (Fig. 5a, b). This growth was more pronounced for the samples deformed at

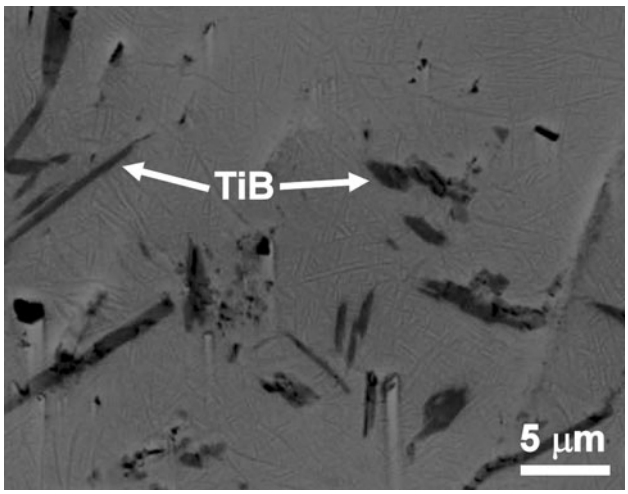

Fig. 4 Backscatter SEM Micrographs of the TZNB alloy deformed and solution treated at 800°C for 1 h followed by air cooling

650°C (Fig. 5b) than at 800°C (Fig. 5a). Tables 2 and 3 summarize the microstructural features of all the heat treated TZN and TZNB samples.

3.2 Anodic polarization

Anodic polarization behaviour of different heat treated TZN samples as measured with respect to saturated calomel electrode (SCE) is shown in Figs. 6 and 7. The corresponding corrosion data are given in Table 4.

In case of deformation and solution treatment at 800°C, the furnace cooled samples showed lower E_{corr} than air cooled samples. On the other hand, the E_{corr} of the water quenched sample was lower than that of the furnace cooled or air cooled samples. Aging of water quenched samples further decreased the E_{corr} value. Among all the samples subjected to deformation and solution treatment at 800°C, the maximum passive current density was observed in case of air cooled samples (Fig. 6a). On the other hand, the aged samples exhibited the lowest passive current density whereas it is slightly higher in case of water quenched samples. The passive current density of the furnace cooled samples is in between air cooled and water quenched samples.

When solution treatment was done at 650°C after deformation at 800°C, an overall increase in E_{corr} values was observed (Fig. 6b). The furnace cooled samples showed lower E_{corr} (−540 mV) than air cooled (−470 mV) or water quenched (−448 mV) samples. Aging of the water quenched sample decreased the E_{corr}. The passive current density of all these heat treated samples varied between 6.3 and 12.6 μA/cm^2 and water quenched samples showed higher passive current density than other heat treated samples.

The E_{corr} values of the samples deformed at 650°C and solution treated at 700°C varied within a narrow range (−470 to −502 mV). The water quenched samples showed

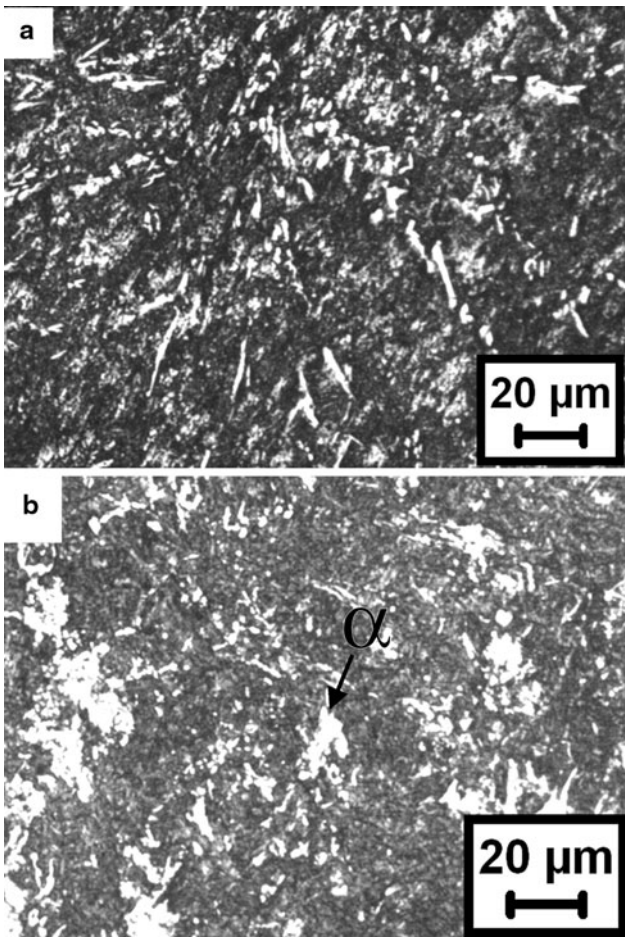

Fig. 5 Microstructures of the TZNB alloy deformed at (**a**) 800°C and (**b**) 650°C, then solution treated at 650°C for 1 h followed by water quenching. Aging at 500°C for 5 h after water quenching

lower E_{corr} than the furnace cooled or air cooled samples (Fig. 7a). Aging of the water quenched sample decreased $E_{corr.}$ The passive current density of the air cooled sample was higher than other heat treated samples. The i_{pass} of furnace cooled and aged samples were comparable whereas water quenched samples showed lower i_{pass}.

After deformation at 650°C, compared to the solution treatment at 700°C, solution treatment at 650°C led to a decrease in E_{corr} value of all the heat treated samples. The furnace cooled sample showed the lowest and water quenched sample gave the highest E_{corr} value (Fig. 7b). In this heat treatment condition the passive current density of all the samples varied between 6.0 and 22.0 μA/cm^2. The water quenched or aged samples showed higher i_{pass} than furnace cooled or air cooled samples.

In general, furnace cooled samples showed lower E_{corr} than air cooled samples. Aging treatment of water quenched samples decreased the E_{corr} value. In most of the cases, the passive current density varied within a narrow range.

Table 2 Microstructural features of the heat treated TZN alloy

Heat treatment			Microstructural features
Hot working temperature (°C)	Solution treatment temperature (°C)	Cooling condition	
800	800	FC	Basket-weave structure (Widmanstätten lath like α) formed from prior β grains
		AC	Fine Widmanstätten α laths within pre-existing β grains
		WQ	Martensite with retained β phase
		WQ & aged	Fine distribution of globular α along pre-existing martensite plates
	650	FC	Primary α and transformed β within β phase. Growth of primary α because of slow cooling
		AC	Primary α and transformed β on a relatively fine scale
		WQ	Primary α and retained β. Partitioning of alloying elements during β to α transformation at 650°C resulting in enrichment of β with Nb which prevents martensite formation
		WQ & aged	Growth of α
650	700	FC	Equiaxed primary α due to recrystallization of elongated α and transformed β
		AC	Equiaxed primary α on a fine scale and transformed β
		WQ	Globular/elongated α and martensite
		WQ & aged	Growth of primary α while retaining the overall morphology of the water quenched samples
	650	FC	Equiaxed primary α due to recrystallization of any elongated α and transformed β. Growth of primary α
		AC	Equiaxed primary α on a fine scale and transformed β
		WQ	No martensite due to partitioning effect. Elongated α due to incomplete recrystallization
		WQ & aged	Equiaxed α

Table 3 Microstructural features of the heat treated TZNB alloy

Heat treatment			Microstructural features
Hot working temperature (°C)	Solution treatment temperature (°C)	Cooling condition	
800	800	FC	Basket-weave α lath and TiB precipitates
		AC	Fine Widmanstätten α laths within pre-existing β grains with precipitates of TiB particles in the matrix
		WQ	Martensite with retained β phase and TiB particles
		WQ & aged	Some growth of α precipitates with precipitation of TiB
	650	AC	Growth of primary α and presence of TiB precipitates in β matrix
		WQ	Some growth of primary α, presence of retained β and TiB particles
		WQ & aged	Higher growth of α with precipitation of TiB
650	650	AC	Growth of the equiaxed primary α and TiB particles in transformed β.
		WQ	No martensite due to partitioning effect. Growth of α phase and precipitation of TiB.
		WQ & aged	Substantial growth of α and precipitates of TiB particles

The anodic polarization curves of the heat treated TZNB alloy are shown in Fig. 8 and the corresponding corrosion data are presented in Table 5.

In case of samples deformed at 800°C and solution treated at the same temperature, compared to the TZN alloy, TZNB alloy showed a small decrease in the E_{corr} value and a substantial increase in passive current density (Fig. 8a).

Solution treatment at 650°C after deformation at 800°C did not change the E_{corr} values of TZNB samples appreciably when compared with the similarly heat treated TZN samples. However, under this heat treatment condition, a

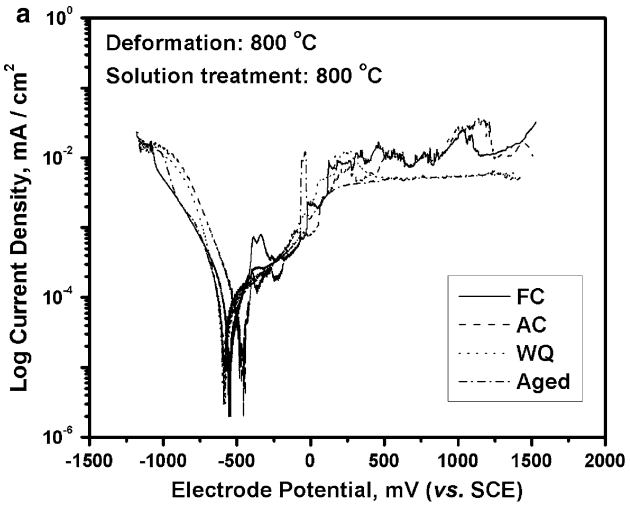

Fig. 6 Anodic polarization behaviour of TZN alloy in Hank's solution. The samples were deformed at 800°C and solution treated for 1 h at (**a**) 800°C and (**b**) 650°C

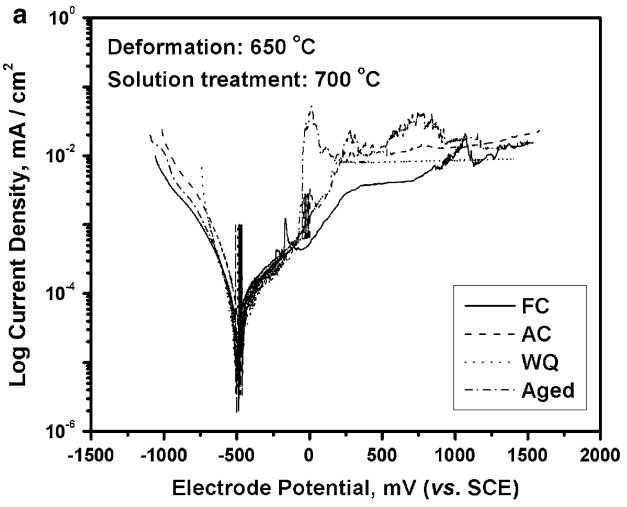

Fig. 7 Anodic polarization behaviour of TZN alloy in Hank's solution. The samples were deformed at 650°C and solution treated for 1 h at (**a**) 700°C and (**b**) 650°C

significant increase in passive current density was observed in boron containing alloy (Fig. 8b).

TZNB samples deformed and solution treated 650°C showed lower E_{corr} values than TZN samples subjected to similar heat treatment conditions. The E_{corr} was found to be lower for aged samples than for air cooled or water quenched samples (Fig. 8c). Here also the passive current density measurement revealed a higher value for TZNB samples than TZN samples.

For any particular solution treatment temperature the variation of E_{corr} of TZNB alloy with respect to heat treatment was found to be similar to that of TZN alloy. Presence of boron did not change the corrosion potential substantially but increased the passive current density of the material significantly. Moreover, no transpassivation was observed in TZN alloy as well as in TZNB alloy.

4 Discussion

In the present study, the passive current density of most of the TZN samples falls in a narrow range. Titanium and its alloys show a tendency to form a stable and tightly adherent protective oxide layer on their surfaces even in solutions with low oxygen contents [4, 5]. This layer protects the underneath material from the aggressive environments [3]. Oliveira et al. [14] have observed that an oxide layer is formed on Ti–13Zr–13Nb and Ti–50Zr alloys in aerated solution also. Semlitsch et al. [24] found that Ti–6Al–7Nb, Ti–6Al-4 V and CP titanium passivated in a deaerated Ringer's solution with the primary passive current density at $\sim 10\ \mu A/cm^2$. In the present study, as soon as the TZN sample is exposed in the Hank's solution a protective surface oxide layer is formed on the surface of the sample and the sample passivates which is also

Table 4 Corrosion potential and passivation parameter obtained from the anodic polarization curves of the heat treated TZN alloy in Hank's solution

Deformation temperature (°C)	Solution treatment temperature (°C)	Cooling conditions	E_{corr} (mV)	i_{pass} (μA/cm^2)
800	800	FC	–535 ± 11	12.6 ± 4.7
		AC	–502 ± 28	41.5 ± 11.7
		WQ	–578 ± 28.4	6.3 ± 3.1
		Aged	–589 ± 21	5.7 ± 1.7
	650	FC	–540 ± 17	6.3 ± 3.8
		AC	–470 ± 37	8.0 ± 0.9
		WQ	–458 ± 20.3	12.6 ± 3.7
		Aged	–523 ± 5.7	7.9 ± 5.2
650	700	FC	–480 ± 5.6	14.6 ± 3.4
		AC	–470 ± 12	22.2 ± 3.2
		WQ	–495 ± 18	8.6 ± 4.5
		Aged	–502 ± 5.1	14.5 ± 6.2
	650	FC	–553 ± 8.3	6.6 ± 2.1
		AC	–512 ± 18.2	6.0 ± 2.2
		WQ	–501 ± 19.5	17.0 ± 2.4
		Aged	–526 ± 24.5	22.0 ± 3.4

reflected in the polarization diagrams (Figs. 6, 7). However, in some cases, the passive current density is relatively high. Surface oxide composition and/or distribution are expected to affect the corrosion behavior of orthopaedic alloys [25]. It has been reported that when alloying elements (except V and Fe) form an oxide they occur as discrete clusters embedded in a titanium oxide matrix [25]. In the present study, the heat treatment in some cases may have led to uneven distribution of the alloying elements in various phases resulting in unstable passive layer formation.

Compared to the furnace cooled or aged samples, the amount of α phase is less in air cooled samples, but at the same time they are finely distributed in the matrix and therefore, the α/β interface area is increased. This accelerates the galvanic corrosion of the material. Raman et al. [26] found that the corrosion potential (E_{corr}) of cp-Ti which consists of single phase α was lower than the α + β type two phase Ti–6Al–7Nb alloy. In the present study also presence of α phase in the microstructure decreases the E_{corr} value. The lower corrosion potential of the furnace cooled or aged sample is associated with the presence of a higher amount of α phase in the matrix. Formation of martensite took place in samples water quenched from a solution treatment temperature of 800°C. Martensite forms by a displacive, shear mechanism of transformation that involves an invariant plane strain (IPS) shape deformation with large shear component. This entails a high amount of strain energy because the shape change has to be accommodated in the parent phase [27]. For example, Ahmed et al. [28] have observed that orthorhombic martensite (α″) produced by quenching the solution treated binary Ti-Nb alloy containing 16–23.4 at% Nb had a strained and highly faulted substructure. The high strain energy associated with the formation of martensite decreased the E_{corr} value of the water quenched samples. On the other hand, absence of any α–β interface decreased the corrosion of the water quenched samples. After aging of the water quenched sample that was solution treated from above β transus, fine precipitates of globular α form and correspondingly, the α–β interface increases. At the same time aging treatment relieves the strain energy associated with martensite in the water quenched sample. Therefore, no appreciable change in corrosion behaviour was observed after aging of the water quenched sample. When solution treatment is done at 650°C martensite is not formed in the matrix. The microstructure consists of α and β phases and there is no strain energy associated with the martensite formation. Thus, no appreciable change in corrosion potential is found between air cooled and water quenched samples. Slow cooling from the solution treatment temperature leads to higher amounts of less noble α phase formation and hence the E_{corr} decreases. During aging, some part of the retained β transforms into α and at the same time α particles grow and thus, the α/β interface area decreases. This has led to a decrease in corrosion current density.

Compared with water quenching from 800°C, water quenching from 700°C led to the formation of less amount of martensite and therefore the associated strain energy was smaller. On the other hand, heavy deformation (>30%) at 650°C (below the β transus) produced worked structure in the material and α phase was nucleated during the plastic deformation. Subsequent annealing in the α + β phase field at 650°C or 700°C followed by water quenching produced

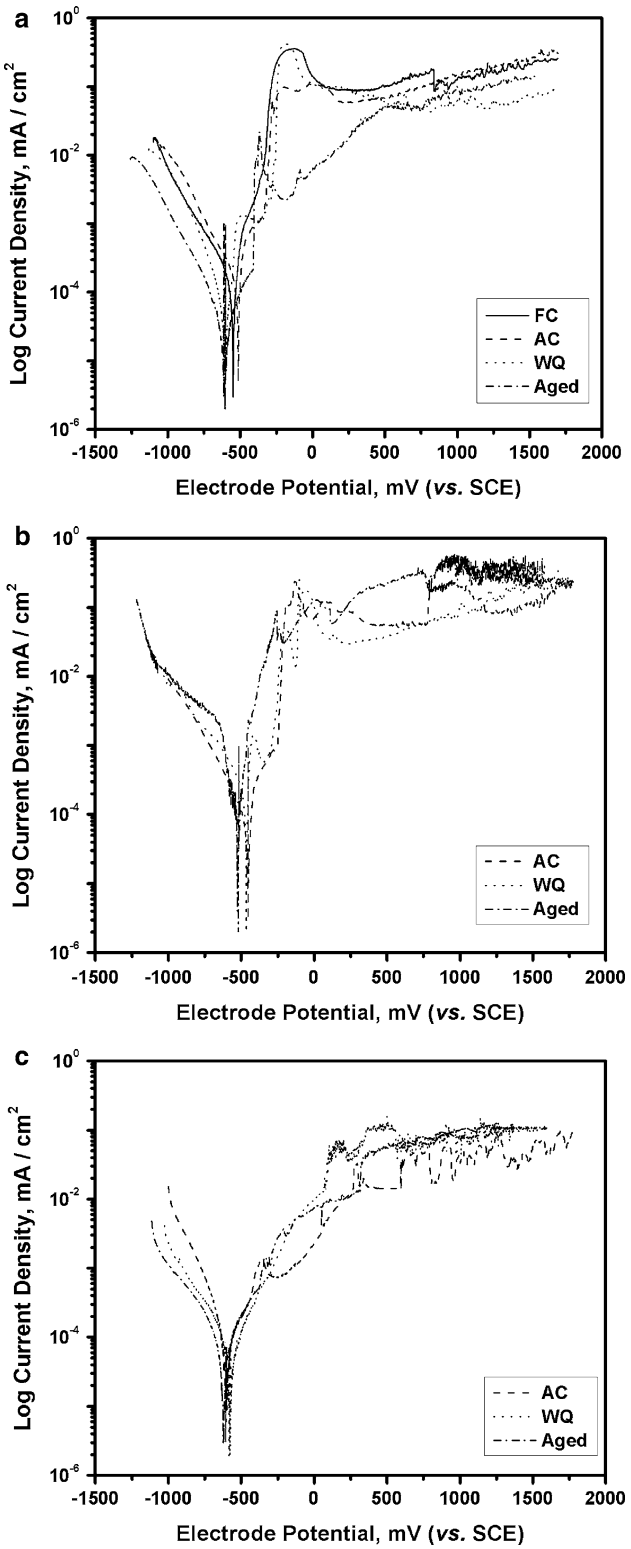

Fig. 8 Anodic polarization behaviour of TZNB alloy in Hank's solution (**a**) deformed and solution treated at 800°C, (**b**) deformed at 800°C and solution treated at 650°C and (**c**) deformed and solution treated at 650°C

elongated α because of incomplete recrystallization of deformed α due to faster cooling. Aging treatment of water quenched sample resulted in the growth of primary α while retaining the overall morphology of the water quenched sample. Therefore, in case of sample deformed at 650°C and solution treated at 700°C presence of elongated α in the microstructure and formation of new α phase from the martensite increase the α/β interface and as a result the corrosion current increases. This effect is more evident for the sample deformed and solution treated at 650°C because here the amount of α phase is relatively high compared with the sample water quenched from 700°C.

Compared to TZN samples, TZNB samples showed slightly lower corrosion potential (E_{corr}) and higher passive current density (i_{pass}). It has been reported in literature that the presence of TiB_2 in Ti increased the primary passivation and the passive currents but did not appreciably affect the corrosion potential and the corrosion behavior of the TiB was similar to that of TiB_2 [29]. In the present study, the addition of boron has resulted in the formation of TiB precipitates in the matrix. Moreover, the precipitation of TiB particles also leads to the refinement of microstructure [30, 31]. The presence of TiB particles in the matrix and the increased α/β interface as a result of the refinement of the microstructure accelerate galvanic corrosion of the material and thus, increase the corrosion. However, in case of samples deformed and solution treated at lower temperature, the growth of α phase decreases the α/β interface area that partially compensates the increase in corrosion due to the presence of TiB particles. This leads to a marginal increase in corrosion of the sample.

In the present investigation, no transpassivation was found in all the TZN and TZNB samples. Oliveira et al. [14] did not find transpassivation and pitting for Ti–6Al–7Nb, Ti–4Nb–15Zr and Ti–13Zr–13Nb alloys in Hank's solution at potential as high as 2 V. Similar observation has been reported on as-cast as well as heat treated Ti–13Zr–13Nb alloy at potentials of up to 8 V in chloride-containing solutions [14]. One should not expect to see transpassive behaviour on this material since none of its components has a higher oxidation state than the one present in the oxide. Therefore, they cannot undergo transpassive dissolution.

5 Conclusions

In the present study, the corrosion behaviour of boron free and boron containing Ti–13Zr–13Nb alloy subjected to different heat treatment conditions was investigated and from the results obtained the following conclusions can be drawn:

Table 5 Corrosion potential and passivation parameter obtained from the anodic polarization curves of the heat treated TZNB alloy in Hank's solution

Deformation temperature(°C)	Solution treatment temperature (°C)	Cooling conditions	E_{corr} (mV)	i_{pass} ($\mu A/cm^2$)
800	800	FC	–564 ± 11	245 ± 16
		AC	–532 ± 26	320 ± 39
		WQ	–589 ± 15	83 ± 18
		Aged	–595 ± 32	130 ± 9
	650	AC	–495 ± 34	249 ± 36
		WQ	–468 ± 18	243 ± 9.5
		Aged	–530 ± 11	278 ± 19
650	650	AC	–594 ± 8	105 ± 13
		WQ	–561 ± 16	97 ± 15.5
		Aged	–621 ± 18	105 ± 23

- Depending on the heat treatment conditions, the microstructure of the heat treated TZN alloy mainly consists of elongated/equiaxed α, β or martensite. Addition of 0.5 wt% B to TZN alloy results in the formation of TiB particles and modifies the α phase.
- In general, furnace cooled TZN sample shows lower E_{corr} than air cooled sample. Water quenching from above or near β transus temperature leads to further decrease in corrosion potential. Aging treatment of water quenched sample decreases the E_{corr} value. In most of the cases, the passive current density varies in a narrow range.
- Presence of boron decreases the corrosion potential and substantially increases the passive current density of TZN alloy and therefore, it deteriorates the corrosion resistance of the TZN alloy.

References

1. López MF, Gulirrez A, Jimnez JA. Surface characterization of new non-toxic titanium alloys for use as biomaterials. Surf Sci. 2001;482–485:300–5.
2. Mändl S, Rader R, Thorwarth G, Krause D, Zeilhofer HF, Horch HH, Rauschenbach B. Investigation on plasma immersion ion implantation treated medical implants. Biomol Eng. 2002;19: 129–32.
3. López MF, Jimnez JA, Gutiérrez A. Corrosion study of surface-modified vanadium-free titanium alloys. Electrochim Acta. 2003;48:1395–401.
4. Okazaki Y, Tateishi T, Ito Y. Corrosion resistance of implants alloys in pseudo physiological solution and role of alloying elements in passive films. Mater Trans JIM. 1997;38:78–84.
5. Leinenbach C, Eifler D. Fatigue and cycle deformation behaviour of surface-modified titanium alloys in simulated physiological media. Biomaterials. 2006;27:1200–8.
6. Geetha M, Mudali UK, Gogia AK, Asokamani R, Raj BD. Influence of microstructure and alloying elements on corrosion behavior of Ti–13Nb–13Zr alloy. Corros Sci. 2004;46:877–92.
7. Aparicio C, Gil FJ, Fonseca C, Barbosa M, Planell JA. Corrosion behaviour of commercially pure titanium shot blasted with different materials and sizes of shot particles for dental implant applications. Biomaterials. 2003;24:263–73.
8. Okazaki Y, Rao S, Ito Y, Tateishi T. Corrosion resistance, mechanical properties, corrosion fatigue strength and cytocompatibility of new Ti alloys without Al and V. Biomaterials. 1998;19:1197–215.
9. Manivasagam G, Mudali UK, Asokamani R, Raj B. Corrosion and microstructural aspects of titanium and its alloys as orthopaedic devices. Corros Rev. 2003;21:125–59.
10. Yu SY, Scully JR. Corrosion and passivity of Ti–13%Nb–13%Zr in comparison to other biomedical implant alloys. Corrosion. 1997;53:965–76.
11. Okazaki Y. A new Ti–15Zr–4Nb–Ta alloy for medical applications. Curr Opi Sol State Mat Sci. 2001;5:45–53.
12. Khan MA, Williams RL, Williams DF. In vitro corrosion and wear of titanium alloys in the biological environment. Biomaterials. 1996;17:2117–26.
13. Khan MA, Williams RL, Williams DF. The corrosion behaviour of Ti–6Al-4 V, Ti–6Al–7Nb and Ti–13Zr–13Nb in protein solutions. Biomaterials. 1999;20:631–7.
14. Oliveira NTC, Ferreira EA, Duarte LT, Biaggio SR, Rocha-Filho RC, Bocchi N. Corrosion resistance of anodic oxides on the Ti–50Zr and Ti–13Zr–13Nb alloys. Electrochim Acta. 2006;51:2068–75.
15. Cai Z, Shafer T, Watanabe I, Nunn ME, Okabe T. Electrochemical characterization of cast titanium alloys. Biomaterials. 2003;24:213–8.
16. Niinomi M, Kuroda D, Fukunaga KI, Morinaga M, Kato Y, Yashiro T, Suzuki A. Corrosion wear fracture of new β type biomedical titanium alloys. Mater Sci Eng A. 1999;263:193–9.
17. Williams DF. Titanium for medical applications. In: Brunette DM, Tengvall P, Texfor M, Thomsen P, editors. Titanium in medicine. New York: Springer; 2001. p. 13–24.
18. Kobayashi E, Doi H, Yoneyama T, Hamanaka H, Gimson IR, Best SM, Shelton JC, Bonfield W. Influence of aging heat treatment on mechanical properties of biomedical Ti–Zr based ternary alloys containing niobium. J Mater Sci Mater Med. 1998;9:625–30.
19. Samuel S, Nag S, Scharf TW, Banerjee R. Wear resistance of laser-deposited boride reinforced Ti–Nb–Zr–Ta alloy composites for orthopedic implants. Mater Sci Eng C. 2008;28:414–20.
20. Zhang X, Lu W, Zhang D, Wu R. In situ technique for synthesizing (TiB + TiC)/Ti composites. Scripta Mater. 1999;41: 39–46.
21. Chen W, Boehlert CJ. The elevated-temperature fatigue behavior of boron-modified Ti–6Al-4 V (wt%) castings. Mater Sci Eng A. 2008;494:132–8.
22. Majumdar P. PhD Thesis. IIT Kharagpur, India. 2009.

23. Majumdar P, Singh SB, Chakraborty M. Wear response of heat-treated Ti–13Zr–13Nb alloy in dry condition and simulated body fluid. Wear. 2008;264:1015–25.
24. Semlitsch MF, Weber H, Streicher RM, Schön R. Joint replacement components made of hot-forged and surface-treated Ti–6Al–7Nb alloy. Biomaterials. 1992;13:781–8.
25. Long M, Rack HJ. Titanium alloys in total joint replacement—a materials science perspective. Biomaterials. 1998;19:1621–39.
26. Raman V, Tamilselvi S, Nanjundan S, Rajendran N. Electrochemical behaviour of titanium and titanium alloy in artificial saliva. Trends Biomater Artif Organs. 2005;18:137–40.
27. Wayman CM, Bhadeshia HKDH. Phase transformations, nondifusive. In: Cahn RW, Haasen P, editors. Physical metallurgy. Amsterdam: Elsevier Science Publishers; 1996. p. 1507–54.
28. Ahmed T, Rack HJ. Martensitic transformations in Ti-(16–26 at%) Nb Alloys. J Mater Sci. 1996;31:4267–76.
29. Bernard S, Covino Jr, Alman DE. Corrosion of titanium matrix composites, Report No.: DOE/ARC-2002-011, Albany Research Center, U.S. Department of Energy, Albany, OR USA.
30. Tamirisakandala S, Bhat RB, Tiley JS, Miracle DB. Grain refinement of cast titanium alloys via trace boron addition. J Mater Eng Perform. 2005;53:1421–6.
31. Cherukuri B, Srinivasan R, Tamirisakandala S, Miracle DB. The influence of trace boron addition on grain growth kinetics of the beta phase in the beta titanium alloy Ti–15Mo–2.6Nb–3Al–0.2Si. Scripta Mater. 2009;60:496–9.